Novel Wide-Range Frequency Offset Estimation and Compensation for Burst-mode CPFSK Upstream Signaling in TDM-Based Digital Coherent PON

Takuya Kanai, Ryo Koma, Masamichi Fujiwara, Jun-ichi Kani, *Senior Member, IEEE*, and Tomoaki Yoshida, *Member, IEEE*

***Abstract*—The burst-mode continuous phase frequency shift-keying (CPFSK) transmitter that combines a directly modulated laser diode, an electro absorption modulator and a semiconductor optical amplifier is attractive as a cost-effective transmitter for phase modulation formats for digital signal processing (DSP)-based coherent passive optical network (PON) upstream signaling. However, since highly accurate wavelength controllers for the transmitters in optical network units (ONUs) create excessive cost burdens, large carrier frequency offsets (CFOs) must be expected. Thus, a CFO compensation method with wide compensation range is required. This paper proposes a novel CFO estimation and compensation method for burst-mode CPFSK signals in upstream PON signaling. The proposed method is based on a simple blind algorithm and does not require any training symbols. We demonstrate wide CFO compensation range, from −12 to 14 GHz, with high receiver sensitivity, less than −42.5 dBm for 10 Gbit/s binary CPFSK signals. This range far exceeds that of the conventional CFO compensation method using a blind algorithm. Moreover, the proposed method can enhance the convergence of finite impulse response (FIR) filters. The feasibility of the proposed CFO compensation technique is successfully demonstrated for burst-mode CPFSK signals.**

***Index Terms*—Passive optical network (PON), time division multiplexing (TDM), continuous phase frequency shift-keying (CPFSK), burst-mode coherent receiver (BMCR), carrier frequency offset (CFO).**

I. Introduction

BROADBAND services are now widely provisioned by the installation of fiber to the home (FTTH). One of the key technologies supporting this massive FTTH deployment is time division multiplexed-passive optical networks (TDM-PONs). TDM-PON can cost-effectively provide broadband optical access services by using a power splitter to share an optical line terminal (OLT) in a central office (CO) and a feeder fiber among a number of optical network units (ONUs) at the subscriber premises. 10G-class optical access network services are now being provided in several countries. Recently, the rapid growth of high-capacity services, such as high-definition video streaming and virtual/augmented reality (AR/VR), is enhancing research into higher-speed TDM-PON systems [1], [2].

As telecom operators are already widely providing FTTH service, determining how to cost-effectively expand the service area of PON-based optical broadband services, reducing the operation expenditure (OPEX) of FTTH service is essential. Furthermore, the capital expenditure (CAPEX) needed to upgrade optical access systems in the future should be reduced so that the cost-effectiveness of higher-speed optical access services approaches that of conventional optical access services. One solution to providing PON-based optical broadband services more cost-effectively is a higher power budget (HPB)-PON system because it can offer longer distances and/or higher splitting ratios. In other words, HPB-PON can increase the number of users accommodated by a single OLT, which reduces the number of OLTs required to provide PON-based broadband services. The service area also can be expanded cost-effectively by using HPB-PON. This will reduce maintenance costs. In addition, the HPB-PON system is an attractive candidate for new network operators who are considering installing new network infrastructures because the initial cost of installing equipment can be reduced.

A technology that can dramatically improve the optical power budget is necessary to realize longer-distance and/or higher-splitting-ratio PON systems. The application of digital signal processing (DSP)-based optical coherent detection combined with optical pre-amplification is an attractive solution because it can significantly raise the power budget of PON systems above that possible with intensity-modulation-direct-detection (IM-DD) [3], [4]. Although coherent reception of IM signals via amplitude-shift-keying (ASK) offers some improvement in receiver sensitivity, phase-shift-keying (PSK) offers higher reception sensitivity because of its longer symbol distances [5]. To realize a PON system based on digital coherent technology, a cost-effective transmitter (Tx) capable of generating phase modulation (PM) signals for ONU installation is necessary. Since the directly modulated laser-diode (DML) can generate PM signals, the DML-based Tx is attractive for realizing such a Tx[6]. We proposed the burst-mode continuous phase frequency shift keying (CPFSK)-Tx composed of a DML, an

Manuscript received 9 September 2022; revised 12 December 2022; accepted 22 December 2022. Date of publication 28 December 2022; date of current version 6 January 2023. *(Corresponding author: Takuya Kanai.)*

The authors are with the NTT Access Network Service Systems Laboratories, Nippon Telegragh and Telephone Corporation, Yokosuka, Kanagawa 239-0847, Japan (e-mail: takuya.kanai.kp@hco.ntt.co.jp; ryou.koma.hf@hco.ntt.co.jp; masamichi.fujiwara.fy@hco.ntt.co.jp; junichi.kani.wb@hco.ntt.co.jp; tomoaki.yoshida.vr@hco.ntt.co.jp).

Digital Object Identifier 10.1109/JPHOT.2022.3232605

electro-absorption modulator (EA) and a semiconductor optical amplifier (SOA)[7].

Since the devices offering high-accuracy wavelength control, such as wavelength lockers, are too expensive for use in the many ONUs, large wavelength variation of the Tx in the ONU must be expected. That induces carrier frequency offset (CFO) which is defined as un-matching of carrier frequencies between the upstream signals output from ONUs and the local oscillator (LO); the CFO induces phase rotation which can degrade receiver sensitivity.

To address this, we have proposed a novel CFO estimation and compensation method based on simple blind algorithm for CPFSK signals; it does not require strict accuracy in training symbol (TS) timing detection [8]. The method was shown to realize a wide compensation range and high receiver sensitivities for 10 Gbit/s CPFSK signals. However, in that study, the proposed CFO compensation method was evaluated using continuous CPFSK signals. The effectiveness of the proposal for burst-mode CPFSK signals was not investigated. Furthermore, CFO was adjusted by controlling the LO's center frequency to maintain the modulation condition of CPFSK Tx. To confirm feasibility, the CFO should be induced by wavelength variation of ONU Tx output.

This paper is an extension of ref. [8] and details experiments on burst-mode CPFSK signals. In addition to confirming the feasibility of the proposed method with burst-mode signals, we experimentally clarify the principle of the proposed CFO compensation method and the effectiveness of the combination of the proposal and the coefficient handover method for the adaptive equalization of finite impulse response (FIR) filtering. In this study, CFO was induced by actual variation of the ONU's Tx wavelength.

The remainder of this paper is organized as follows. Section II briefly details the concept of the digital coherent based PON system for higher-splitting ratios, and issues with upstream burst-mode coherent reception are described. Section III describes the burst-mode CPFSK Tx and a proposed novel CFO estimation and compensation method based on simple algorithm that does not require any TSs. Section IV introduces our experimental setup and results of a feasibility study on the proposed CFO compensation method using binary 10 Gbit/s burst-mode CPFSK signals. Finally, Section V concludes the paper.

II. Issues in High Power Budget PON Systems Based on Digital Coherent Technology

A. High Power Budget PON Systems

In PON systems, an OLT placed in a CO is connected to multiple ONUs in subscriber premises via optical splitters and feeder fiber. Since the IM-DD scheme is applied for both upstream and downstream signals in current PON systems, transmission distance and splitting ratio are usually limited to 20 km and 32, respectively. The power budget defined by Tx output power and receiver sensitivity of receiver (Rx) determines transmission distance and splitting ratio of the system. The cost-effectiveness of an optical access system can be efficiently enhanced by improving the power budget which allows the number of users accommodated in each OLT to be increased. The HPB-PON system enables us service more ONUs with fewer OLTs. Thus, OPEX can be reduced by improving the power budget.

To realize the HPB-PON system cost effectively, optical amplifiers can be used for post/pre-optical amplification at the OLT side [9]. This configuration is more cost-effective than setting an optical amplifier in each ONU, since the optical amplifiers can be shared by the many users accommodated by the OLT. Post-amplification of downstream signals by an optical fiber amplifier, such as an erbium doped fiber amplifier (EDFA), increases the launched power from the OLT and improves the downstream power budget. By using an EDFA, a power budget of more than 50 dB was achieved for 10 Gbit/s IM signals in the C-band [10]. For upstream signals, unfortunately, the effectiveness of the pre-amplifier in improving the received sensitivity is limited due to the large impact of the amplified spontaneous emission (ASE) generated by the optical amplifier for a weak received power. Offsetting such low effectiveness in the upstream reception can be realized by applying digital coherent detection assisted by optical pre-amplification because much higher Rx sensitivity can be achieved than is possible with direct detection [11]. We have proposed a TDM-PON system based on digital coherent technology and demonstrated a symmetric 10G-class PON system with a power budget of more than 50 dB in order to realize 40 km reach and 2048 user accommodation [12]. In this work, we also target a 10-Gbit/s class PON system that can achieve power budget of 50 dB.

Fig. 1 shows a schematic of our TDM-PON system based on digital coherent technology. Since the post-amplification assisted IM-DD scheme is adopted for downstream transmission, the ONU receiver configuration is simplified. On the other hand, PM is applied to the ONU Tx, and the upstream signals are detected by a DSP-based optical coherent detection scheme set in the OLT. That configuration can greatly increase the power budget of upstream signals.

The major technical challenge in applying digital coherent detection is detecting the upstream burst-mode signals. The optical powers of the upstream burst signals received at the OLT Rx are different. Since this power variation induces a variation in signal amplitude input into the ADC after intradyne coherent receiver (ICR), the ADC's dynamic range cannot be fully utilized. Large quantization error occurs if the received power is low, and a receiver sensitivity of the ICR can be degraded. Using an auto-level-controlling (ALC)-EDFA as a pre-amplifier followed by ICR yields coherent reception with wide dynamic range [13]. However, DSP-based equalization must be optimized burst by burst because the signal distortion depends on the characteristics of the ONU Tx and chromatic dispersion, which depends on optical fiber length. To compensate these differences in burst-mode upstream signals, the DSP-based equalizer in the OLT must have very short response time. So far, we have demonstrated a symmetric 10-Gbit/s 40-km reach DSP-based HPB TDM-PON system; in conjunction with a coefficient handover method, it yielded real-time burst-mode coherent reception as the convergence time of tap coefficients for the adaptive equalization of each burst frame was reduced. High receiver sensitivity of −45.1 dBm was achieved after 40 km transmission for burst-mode

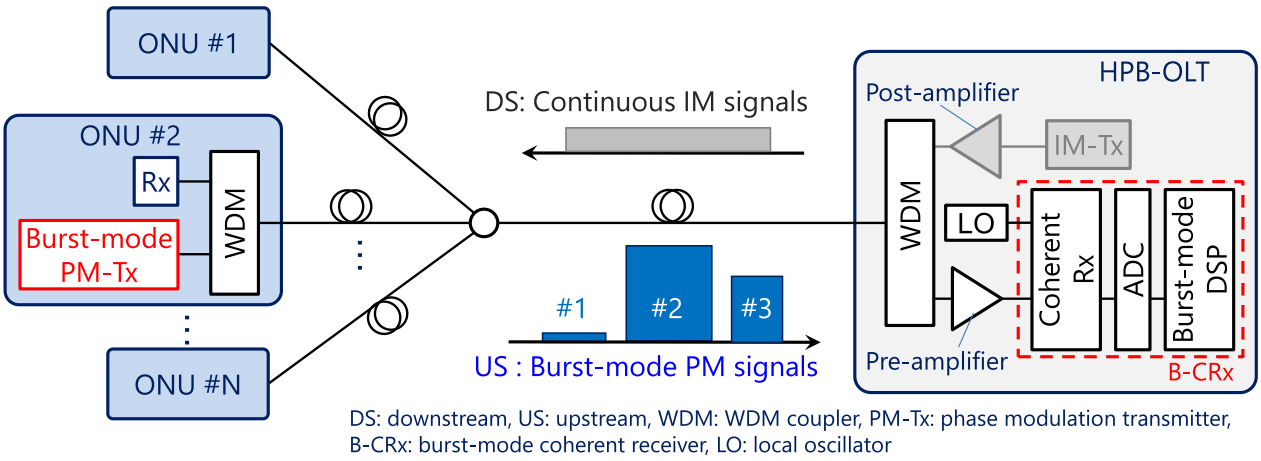

Fig. 1. Schematic of DSP based optical coherent PON.

upstream 10 Gbit/s binary-phase-shift-keying (BPSK) signals [12]. As described in [12], the carrier frequency of the LO and Tx were matched, and the experiment was conducted without CFO. However, to fully verify the reception of burst upstream signals in a DSP-based PON system, CFO compensation is an issue that must be addressed. In the next section, we describe our proposed CFO compensation method.

B. Target Value of the Compensation Range of CFO

The burst-mode signals output from ONUs are received by the ICR in the OLT of the digital coherent PON, as shown in Fig. 1. The CFO due to disparate carrier frequencies between the upstream signals output from the ONUs and the LO in OLT induces phase rotation on the I-Q plane. The value of the phase rotation due to CFO depends on CFO value. The signal cannot be decoded when the CFO value exceeds the processing performance of the DSP. Therefore, a CFO compensation technique is necessary. Two important CFO compensation abilities are essential. The first one is high-speed response because CFO of each upstream burst-mode signal must be compensated within a short preamble. The feed-forward algorithm is better than the feedback to obtain fast convergence for CFO compensation. To shorten the preamble of the upstream burst signals, a blind algorithm is more suitable because it does not need any extra signals for CFO estimation, such as a TS. The second ability is wide CFO compensation range. It is deemed impossible to implement a cost-effective ONU Tx that offers sufficiently accurate wavelength control. Thus, large variation in ONU carrier frequencies is expected, necessitating a wide CFO compensation range.

The most popular CFO compensation technique is based on the M-th power algorithm and is effective for burst signal detection because it uses a blind algorithm with feed-forward control [14]. However, the CFO compensation range for M-ary phase shift keying (M-PSK) signals with baud-rate of B is limited to $\pm B/(2M)$. For instance, the CFO compensation range is limited to $\pm$2.5 GHz for 10 Gbit/s BPSK signals. If CFO value exceeds that range, the correct CFO value cannot be estimated, and signal decoding fails. To determine the target CFO compensation range, we refer to the maximum value of center frequency error of an ONU Tx specified the maximum tuning error (MTE) in the next generation (NG)-PON2 [15]. The MTE is the maximum differential spectral distance of the actual wavelength from the nominal center of the wavelength channel and is determined by the nominal central frequency, which is specified by relationship between the maximum spectral excursion (MSE) and a minimum single-sided spectral width at 15 dB down ($\Delta\omega_{15\mathrm{dB}}$), as shown in Fig. 2. The relationship between MTE and MSE is defined as;

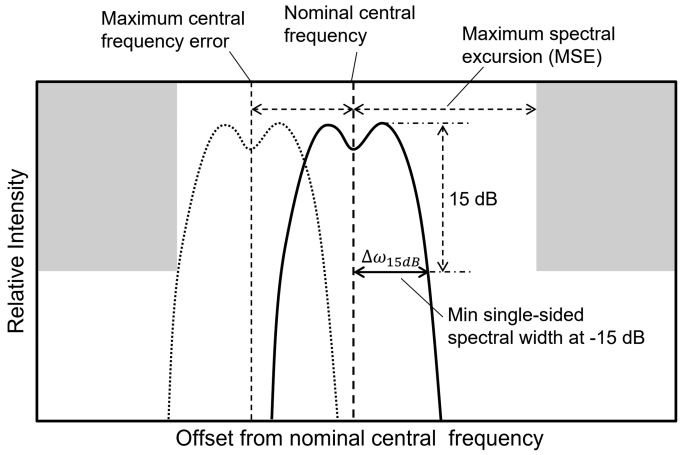

Fig. 2. Maximum tuning error for CPFSK Tx.

$$\mathrm{MTE} = \mathrm{MSE} - \Delta\omega_{15\mathrm{dB}} \tag{1}$$

In NG-PON2, typically, $\Delta\omega_{15\mathrm{dB}}$ is assumed to be equal to the data rate in Hz (= 10 GHz for 10 Gbit/s), so the MSE value is $\pm$20 GHz for 100-GHz channel spacing [15]. Hence, the MTE value is 10 GHz for a 10-Gbit/s signal. This work thus targets the CFO compensation range of $\pm$10 GHz, which is equal to the MSE value specified in NG-PON2.

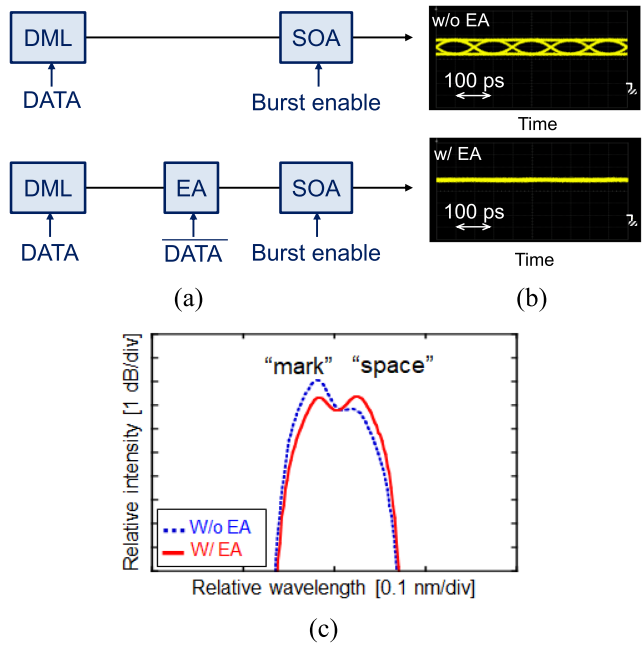

Fig. 3. (a) Configuration of burst-mode CPFSK Tx w/o (top) and w/ (bottom) EA modulator, (b) waveforms output from Tx w/o (top) and w/ (bottom) EA and (c) output spectra from Tx w/o (blue) and w/ (red) EA.

III. Upstream Burst Signals Based on CPFSK

A. Cost-Effective Burst-Mode CPFSK Tx for ONU

CPFSK is a well-known technique for converting frequency modulation (FM) to PM, and can be directly implemented by a DML without any expensive MZMs[16], [17]. Thus, CPFSK is suitable for the ONU Tx since a simple ONU configuration is essential. Fig. 3(a) shows the burst-mode CPFSK Tx configurations we have proposed [7]. CPFSK signals are generated at the DML; the SOA operates as a shutter for burst frame modulation [18]. In general, burst-mode operation of DML induces undesirable frequency drift due to self-heating [19], [20]. The proposed configuration has the benefit of preventing undesirable frequency drift due to self-heating under burst-mode operation of the DML. On the other hand, the CPFSK signals generated by using the upper configuration in Fig. 3(a) contains unnecessary IM components, which lower receiver sensitivity due to signal-noise-to-ratio (SNR) degradation in the space "0" level of the received signals. The EA is used for improving receiver sensitivity, as shown in the lower figure of Fig. 3(a). The DFB-LD and the EA are modulated by data and inverted data signals, respectively. As a result, unnecessary IM components are eliminated (see Fig. 3(b) and (c)). The use of the EA and the SOA may appear to make the Tx configuration more complicated. However, EADFBs monolithically integrated with SOAs can be expected to become commercially available in the near future [21].

Fig. 4 shows sampled constellations of CPFSK signals. Sampled signals after ADC contain phase noise which induces phase rotations on the I-Q plane (Fig. 4(a)). 1-bit delay ($\sim 1/2h$ symbol, h is modulation index) detection cancels the phase noise and so

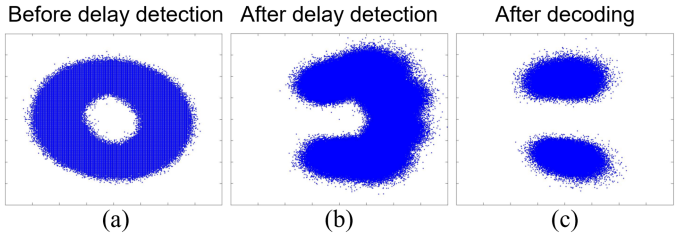

Fig. 4. Received constellations (a) before and (b) after delay detection and (c) after decoding.

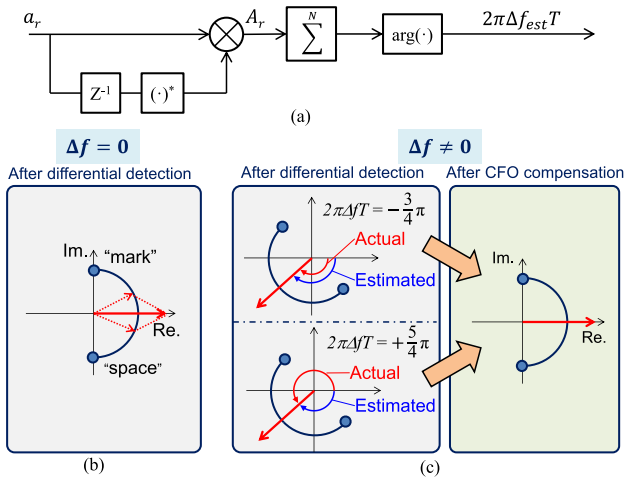

Fig. 5. Proposed CFO estimation method. (a) Block diagram of proposed method. (b) Example of received constellations after 1-bit delay detection. (c) Example of the proposal with CFO of $-3/4\ \pi$ and $+5/4\ \pi$.

yields U-shape constellation (see Fig. 4(b)). Note that, Fig. 4 shows constellations without CFO. This is then decoded to yield binary data, as shown in Fig. 4(c)

B. Proposed CFO Compensation Method for Burst CPFSK Signal

For the burst-mode upstream signals, a method that can compensate their CFO within a short preamble is required. To realize wide CFO compensation range for burst-mode CPFSK signals, we investigate a novel CFO compensation technique. It is based on a simple blind algorithm that does not require either any TS or high-accuracy timing detection. Thus, it can realize quick enough response time to permit the use of short preambles.

Fig. 5 shows a block diagram of the proposed method. The CPFSK signals after 1-bit delay detection, A_r, yield U-type constellations as shown in Fig. 5(b). When CFO (Δf) equals zero, the "mark" and "space" samples lie on the imaginary axis. On the other hand, if Δf does not equal to zero, the same "mark" and "space" samples are rotated on the I-Q plane (Fig. 5(c)). Here, the rotation angle is given by $2\pi\Delta fT$, where T is the delay period ($\sim 1/2h$ symbol) used in 1-bit delay detection. The rotation is clearly visible in the I-Q plane thanks to the U-shape constellations, thus by calculating the vector summation of A_r, CFO, Δf_{est}, is estimated

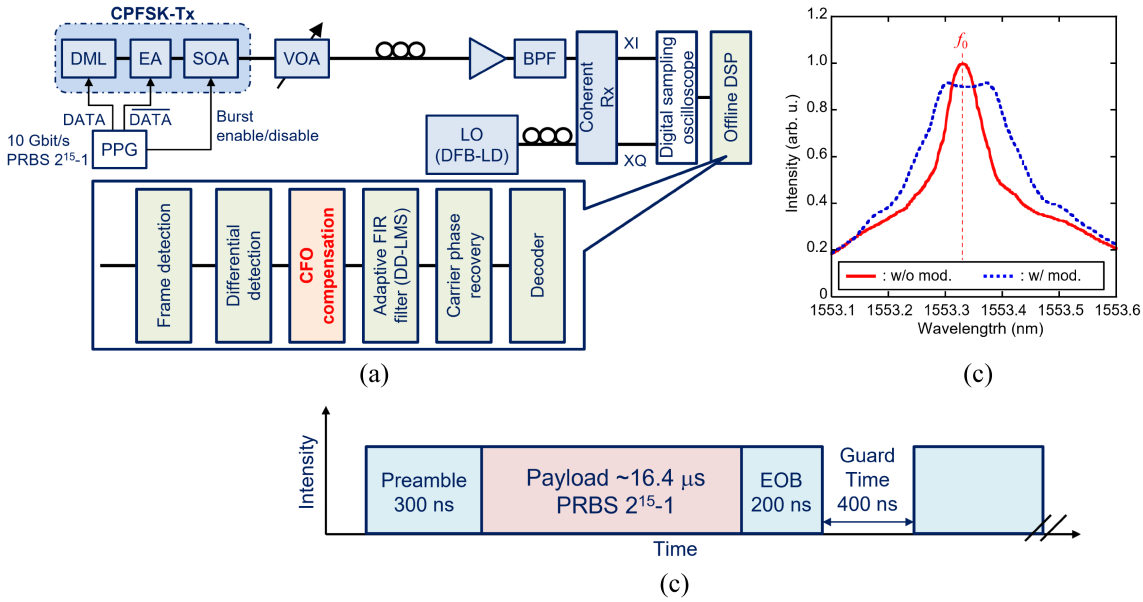

Fig. 6. (a) Experimental setup and (b) output spectrum from EA w/ and w/o modulation. (c) The burst signal sequence.

to be

$$\Delta f_{est} = \frac{arg\left[\sum_N A_r\left(t\right)\right]}{2\pi T} \tag{2}$$

where N is the number of averaged samples. Here, Δf_{est}, is usually chosen within $2\pi\Delta fT$ of $\pm\pi$. For example, Fig. 5(c) illustrates the cases in $2\pi\Delta fT$ of -3/4π (within $\pm\pi$) and +5/4π (beyond $\pm\pi$). When $2\pi\Delta fT$ is -3/4π, Δf_{est} coincides with the actual CFO, thus the rotated constellation can be properly compensated. On the other hand, when $2\pi\Delta fT$ is +5/4π, Δf_{est} does not match to the actual CFO. However, the rotated constellation can still be successfully compensated by using the wrong estimation value since the rotated constellation and the estimated CFO for the case of 5/4π coincide with those for the case of -3/4π.

As a result, the signals are successfully decoded in both situations. We can expect the proposal to offer full-range frequency compensation regardless of the symbol rate in the absence of limitations imposed by the characteristics of electronic and optoelectronic devices used.

The proposal is a blind CFO estimation method that uses the U-shape constellation of CPFSK. However, even for modulation formats that have ring-shape constellations, such as QPSK, the proposal can estimate CFO from vector summation by using a training symbol that yields an asymmetric constellation after differential detection [22].

IV. Experiment and Results

This section describes the results of an experiment on the CFO compensation range of the proposed technique applied to burst mode upstream signals. Fig. 6(a) shows the experimental setup used. The CPFSK Tx consists of a DML, an EA and an SOA. 10 Gbit/s non-return to zero (NRZ) signals with pseudo random bit sequence pattern (PRBS) of $2^{15}-1$ was input to the DML and the EA. The modulation index h was set to 0.8. EA output was sent to the SOA to operate it as a burst shutter and output power of CPFSK-Tx was +8.0 dBm. The Tx output signal was sent to the Rx side via a variable optical attenuator (VOA), an EDFA with noise figure of 4.9 dB, and an optical band-pass filter (BPF) as a WDM filter. The Rx consisted of a LO, a commercially available polarization-diversity coherent receiver with a bandwidth of 20 GHz, a digital sampling oscilloscope (DSO), and a DSP. In the PON systems installed in the field, the state-of-polarization (SOP) can fluctuate burst-by-burst. That fluctuation in SOP can be compensated by DSP using feed-forward methods, such as maximal-ratio combining [11]. In this study, to confirm the feasibility of our proposal, we assumed that the SOP fluctuation can be compensated by DSP using feed-forward compensation, and the optical signals input to the Rx were taken to be aligned to the polarization state of the LO light. The received I-Q signals were sampled by the DSO at 50 GS/s and demodulated by offline DSP consisting of burst frame detection based on auto-correlation, 1-bit delay differential detection, the proposed CFO compensation ($N = 1024$), an adaptive 15-tap finite impulse response (FIR) filter based on a decision-directed least mean square (DD-LMS) algorithm, carrier phase recovery using the M-th power method (M = 2), and a decoder. The linewidths of the DML and the LO were 16 MHz and 100 kHz, respectively. In this study, we used the coefficient handover method for an adaptive FIR filter demonstrated in Ref. [12], [23]. Here, calculations of FIR filter coefficients were performed every 80 symbols to effect realistic DSP with processing frequency of 125 MHz.

Fig. 6(b) shows spectra output from the DML with and without modulation. Since the modulated spectra was broadened (blue line in Fig.(b)), it is difficult to define the center frequency. To accurately measure the CFO value, we defined the CFO as the difference in center frequencies between LO and DML without modulation (red line in Fig. 6(b)). The center frequency of DML, f_0, was set to 193.00 THz (1553.33

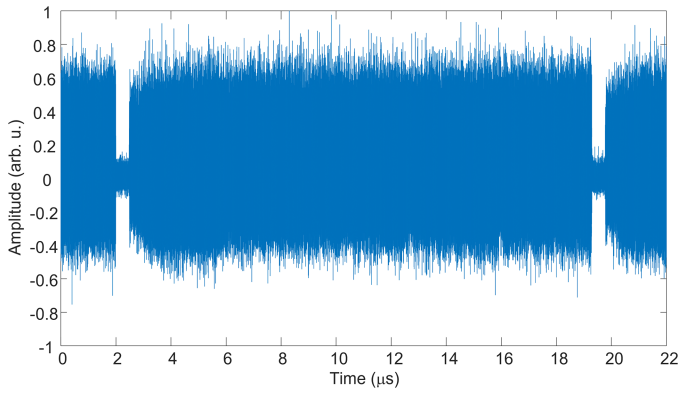

Fig. 7. Received upstream burst-signal.

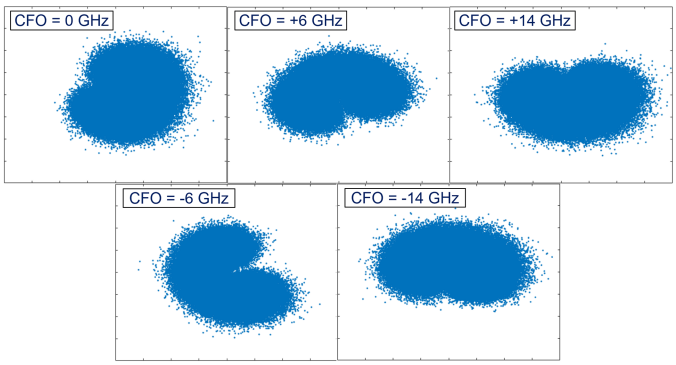

Fig. 8. Received constellations after delay detection on received power of −38 dBm when CFOs are 0 GHz, +6 GHz, +14 GHz, -6 GHz, and −14 GHz, respectively.

nm), and CFO value was set by controlling f_0 via DML temperature.

Fig. 6(c) and Fig. 7 show the configuration of transmitted burst frames and received burst-mode CPFSK signals, respectively, after coherent Rx; the signals contained a preamble of approximately 300 ns, a payload of 16.4 μs (163840 bits with a PRBS of $2^{15}-1$) and an end of burst (EOB) of 200 ns. A guard time of 400 ns was used to separate burst signals.

Fig. 8 shows received constellations after 1-bit delay differential detection for CFO values of 0 GHz, +6 GHz, +14 GHz, −6 GHz, and −14 GHz. Phase rotation is evident according to the CFO value. The relationship between actual CFO values and CFO values estimated by the proposed method is shown in Fig. 9. The actual CFO value was measured by using a wavelength meter with a resolution of 0.1 GHz. In this study,v since the modulation index is 0.8, the phase rotation due to CFO corresponds to $\pm\pi$ when CFO is $\pm$8 GHz. For example, while the actual CFO is +14 GHz, the estimated CFO is about −4 GHz. As described in Section III-B, it is expected that CFO values beyond $\pm\pi$ can be compensated. In this case, estimated CFO was around −4 GHz, as shown in Fig. 9. This value corresponds to -π/2. This means that the proposed method can compensate CFO values beyond $\pm\pi$. The actual and estimated CFO values were different because of a low SNR and non-uniformity of the noise in mark and space. Although the constellation after

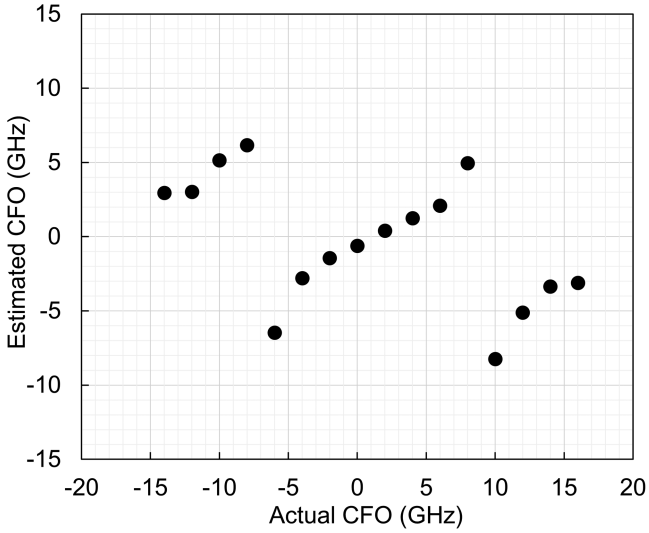

Fig. 9. Relationship between actual CFO value and estimated CFO by the proposed method.

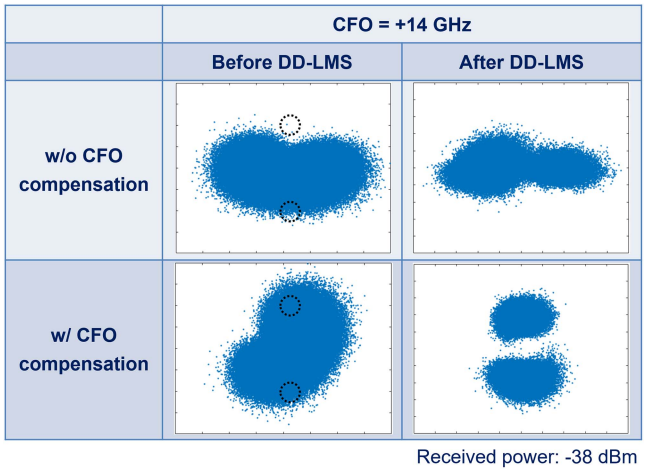

Fig. 10. The constellations decoded by DD-LMS w/ and w/o CFO compensation when CFO = +14 GHz.

CFO compensation is slightly rotated after CFO compensation by using the estimated value, the rotation is small enough to be compensated by the FIR filter.

Fig. 10 shows the results of the constellations after the LMS with and without the proposed CFO compensation. These results were obtained when the received power and the CFO value were set to −38 dBm and +14 GHz, respectively. In this study, we applied a DD-LMS based FIR filter which minimizes the Euclidean distance for mark and space shown as the dashed circles in Fig. 10. Since the CFO value of +14 GHz corresponds to +3/2π, the Euclidean distance to the mark and space of the received signal are almost equivalent. In such cases, the FIR filter yielded the wrong direction of “marks” and “spaces”. Then, the signal decoding to binary data after equalization failed. On the other hand, the signal was successfully decoded with the use of CFO compensation. Thus, the proposed CFO compensation method enhances the adaptive equalization of the DSP-based FIR filter to

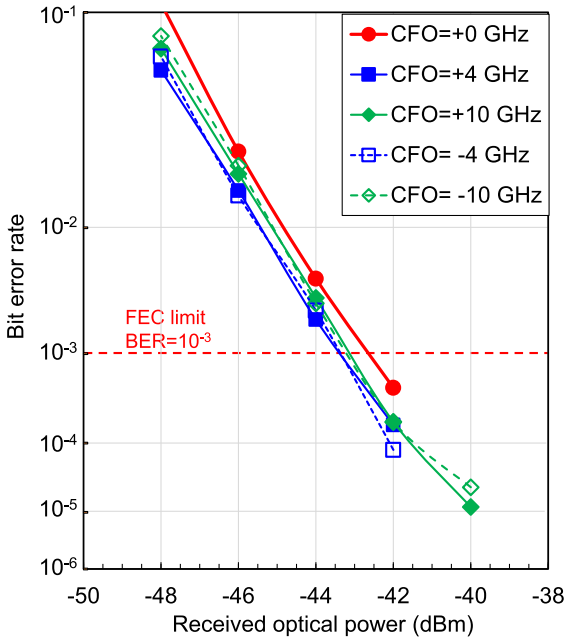

Fig. 11. Results of BER measurement w/ proposed CFO compensation when CFO = 0, −4, −10, +4 and +10 GHz, respectively.

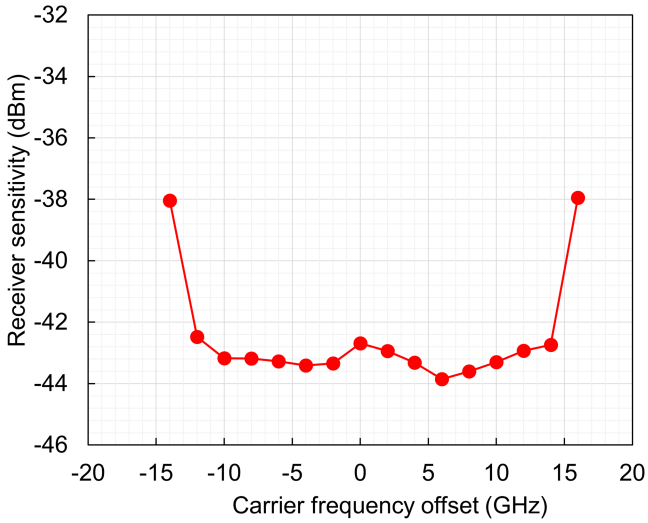

Fig. 12. Receiver sensitivity against CFO.

realize burst-mode coherent reception in digital-coherent-based PON systems. On the other hand, the constellation after CFO compensation was slightly rotated. Since the bandwidth of the receiver used in this study was about 20 GHz, the signal on the higher frequency side was degraded when the CFO value was large. As a result, an imbalance occurred between the intensity components in Mark and Space and it impossible to accurately estimate the CFO value.

Fig. 11 shows the measure BER with the proposed CFO compensation method when CFO were 0, −4, −10, +4 and +10 GHz, respectively. In this study, we assumed the use of Reed-Solomon (255, 223) as adopted by 10G-EPON and define the input power at BER = 10^{-3} as the receiver sensitivity [24]. The penalty due to CFO was negligible, and receiver sensitivity of less than −43 dBm was achieved with the proposed CFO compensation. Fig. 12 plots receiver sensitivity versus the CFO value. High receiver sensitivities, better than −42.5 dBm, were obtained for the CFO range of −12 to +14 GHz, although sensitivities were slightly degraded by the bandwidth limitation of the coherent receiver for large CFO values. Consequently, the power budget of 50.5 dB in the CFO value from −12 to +14 GHz was achieved by using the proposed CFO compensation method. This CFO compensation range is more than 5 times that of the conventional blind method, such as the *M*-th power method. The range depends on the spectral width of the DML output (8 GHz for $h = 0.8$) and receiver bandwidth (20 GHz). Thus, the measured compensation range is eminently practical.

The proposed scheme can enhance future optical access systems. For example, it is expected that the bandwidths of receiver and ADC will increase with advances in technology. This will enable us to use receivers and ADCs that have wider bandwidth than the symbol rate, and the CFO compensation range using the proposed method will be widened. That means the wavelength accuracy requirement of the ONU's Tx can be relaxed for higher-speed PON systems. This yields future optical access systems with more cost-effective Tx configurations.

V. Conclusion

In order to realize a cost-effective upstream Tx for TDM-based digital coherent PONs, we proposed a technology that offers wide CFO compensation range for burst-mode CPFSK upstream signals; it relaxes the wavelength stability required of Tx in the ONUs. This paper detailed and experimentally demonstrated a novel CFO estimation and compensation technique based on a simple algorithm for burst-mode CPFSK signals, that does not require TS or accurate timing detection. The feasibility of the proposed method for burst-mode upstream CPFSK signals was confirmed. The proposed method realized the wide compensation range of ±13 GHz with high receiver sensitivities of under −42.5 dBm for 10 Gbit/s burst-mode CPFSK signals. Furthermore, the proposed method was able to enhance the convergence of the LMS-based FIR filter. The combination of the coefficient handover method and the proposed CFO compensation method enables the upstream burst signals to use the short preamble length of 300 ns. We believe that our proposed CFO compensation method is effective for even higher speed signals because higher speed optical devices, such as photo receiver, ADC, will enhance the CFO compensation range of our proposed method.

References

[1] D. Zhang, D. Liu, X. Wu, and D. Nesset, "Progress of ITU-T higher speed passive optical network (50G-PON) standardization," *J. Opt. Commun. Netw.*, vol. 12, no. 10, pp. D99–D108, Oct. 2020, doi: 10.1364/JOCN.391830.

[2] N. Suzuki, S. Yoshima, H. Miura, and K. Motoshima, "Demonstration of 100-Gb/s/λ-Based coherent WDM-PON system using new AGC EDFA based upstream preamplifier and optically superimposed AMCC function," *J. Lightw. Technol.*, vol. 35, no. 8, pp. 1415–1421, Apr. 2017, doi: 10.1109/JLT.2016.2646344.

[3] R. Koma et al., "Demonstration of real-Time burst-Mode digital coherent reception with wide dynamic range in DSP-Based PON upstream," *IEEE J. Lightw. Technol.*, vol. 35, no. 8, pp. 1392–1398, Apr. 2017.

[4] J. Zhang, Z. Jia, M. Xu, H. Zhang, and L. A. Campos, "Efficient preamble design and digital signal processing in upstream burst-mode detection of 100G TDM coherent-PON," *J. Opt. Commun. Netw.*, vol. 13, no. 2, pp. A135–A143, Feb. 2021.

[5] A. W. Davis, M. J. Pettitt, J. P. King, and S. Wright, "Phase diversity techniques for coherent optical receivers," *IEEE J. Light. Technol.*, vol. 5, no. 4, pp. 561–572, Apr. 1987, doi: 10.1109/JLT.1987.1075539.

[6] I. N. Cano, A. Lerin, V. Polo, and J. Prat, "Direct phase modulation DFBs for cost-Effective ONU transmitter in udWDM pons," *IEEE Photon. Technol. Lett.*, vol. 26, no. 10, pp. 973–975, May. 2014.

[7] M. Fujiwara et al., "Performance evaluation of CPFSK transmitters for TDM-Based digital coherent PON upstream," in *Proc. Opt. Fiber Commun. Conf.*, 2017, pp. 1–3.

[8] T. Kanai et al., "Wide-Range frequency offset compensation for CPFSK used as RDAM-Based Digital Coherent PON's upstream signals," in *Proc. Eur. Conf. Opt. Commun.*, 2018, pp. 1–3, doi: doi: 10.1109/ECOC.2018.8535224.

[9] K. Taguchi, "Long-Reach and high-Splitting technologies for 40-Gbit/s-Class λ-tunable TWDM-PON," in *Proc. Opt. Fiber Commun. Conf.*, 2016, pp. 1–3.

[10] Z. Li, L. Yi, and W. Hu, "Comparison of downstream transmitters for high loss budget of long-reach 10G-PON," in *Proc. Opt. Fiber Commun.*, 2014, pp. 1–3.

[11] K. Kikuchi and S. Tsukamoto, "Evaluation of sensitivity of the digital coherent receiver," *J. Light. Technol.*, vol. 26, no. 13, pp. 1817–1822, Jul. 2008.

[12] T. Kanai et al., "Symmetric 10 gbit/s 40-km reach DSP-based TDM-PON with a power budget over 50 dB," *Opt. Exp.*, vol. 29, no. 11, pp. 17499–17509, 2021, doi: 10.1364/OE.421917.

[13] R. Koma, M. Fujiwara, J. I. Kani, K. I. Suzuki, and A. Otaka, "Wide dynamic range burst-mode digital coherent detection using fast ALC-EDFA and pre-calculation of FIR filter coefficients," in *Proc. Opt. Fiber Commun. Conf. Exhib.*, 2016, pp. 1–3.

[14] A. Leven, N. Kaneda, U. Koc, and Y. Chen, "Frequency estimation in intradyne reception," *IEEE Photon. Technol. Lett.*, vol. 19, no. 6, pp. 366–368, 2007.

[15] *40-Gigabit-Capable Passive Optical Networks 2 (NG-PON2): Physical Media Dependent (PMD) Layer Specification*, ITU-T Rec. G.989.2, International Telecommunications Union, Geneva, Switzerland, Dec. 2014.

[16] K. Iwashita and T. Matsumoto, "Modulation and detection characteristics of optical continuous phase FSK transmission system," *J. Lightw. Technol.*, Vol. 5, no. 4, pp. 452–460, (1987).

[17] Y. Nakanishi et al., "Novel optical quaternary minimum shift keying technology with direct modulation of conventional DFB laser and digital coherent detection," in *Proc. IEEE Photon. Conf.*, 2012, pp. 238–239.

[18] K. Taguchi et al., "High output power and burst extinction ratio λ-tunable ONU transmitter using burst-mode booster SOA for WDM/TDM-PON," *J. Opt. Commun. Netw.*, vol. 7, no. 1, pp. 1–7, Jan. 2015.

[19] R. Bonk et al., "The underestimated challenges of burst-mode WDM transmission in TWDM-PON," *Opt. Fiber Technol.*, vol. 26, pp. 59–70, 2015.

[20] W. Poehlmann, D. V. Veen, R. Farah, T. Pfeiffer, and P. Vetter, "Wavelength drift of burst-Mode DML for TWDM-PON," *J. Opt. Commun. Netw.*, vol. 7, no. 1, pp. A44–A51, Jan. 2015.

[21] T. Shindo et al., "High modulated output power over 9.0 dBm with 1570-nm wavelength SOA assisted extended reach EADFB laser (AXEL)," *J. Sel. Topics Quantum Electron.*, vol. 23, no. 6, pp. 1–7, Mar. 2017.

[22] R. Koma, M. Fujiwara, R. Igarashi, K. Hara, J.-I. Kani, and T. Yoshida, "Novel data-aided carrier frequency offset compensation methods using asymmetric-shape constellations for burst-mode coherent reception," in *J. Lightwave Tech.*, vol. 41, no. 1, pp. 159–168, Jan. 1, 2023, doi: 10.1109/JLT.2022.3215193.

[23] R. Koma et al., "Burst-Mode digital signal processing that pre-Calculates FIR filter coefficients for digital coherent PON upstream," *IEEE J. Opt. Commun. Netw.*, vol. 10, no. 5, pp. 461–470, May. 2018.

[24] *IEEE Standard for Information technology– Local and metropolitan area networks– Specific requirements– Part vol. 3: CSMA/CD Access Method and Physical Layer Specifications Amendment 1: Physical layer Specifications and Management Parameters for 10 gb/s Passive Optical Networks*, IEEE Standard 802.3av-2009 (Amendment to IEEE Standard 802.3-2008), Oct. 2009, doi: 10.1109/IEEESTD.2009.5294950.